ResearchGate

See discussions, stats, and author profiles for this publication at:
https://www.researchgate.net/publication/239693192

Photodissociation of vibrationally excited CH3Cl: Modification of the dissociation dynamics

ARTICLE *in* CHEMICAL PHYSICS LETTERS · SEPTEMBER 1997

Impact Factor: 1.9 · DOI: 10.1016/S0009-2614(97)00783-5

CITATIONS
30

READS
5

2 AUTHORS, INCLUDING:

Paul J Dagdigian
Johns Hopkins University
323 PUBLICATIONS **6,131** CITATIONS

SEE PROFILE

Available from: Paul J Dagdigian
Retrieved on: 23 January 2016

5 September 1997

ELSEVIER

Chemical Physics Letters 275 (1997) 499–505

CHEMICAL PHYSICS LETTERS

Photodissociation of vibrationally excited CH_3Cl: modification of the dissociation dynamics

H. Mark Lambert, Paul J. Dagdigian

Department of Chemistry, The Johns Hopkins University, Baltimore, MD 21218-2685, USA

Received 12 May 1997; in final form 26 June 1997

Abstract

Vibrationally excited CH_3Cl is prepared by laser excitation in the fourth C–H stretch overtone transition and photodissociated at fixed wavelengths near 238 nm which also probe the $Cl(^2P_{3/2})$ and $Cl(^2P_{1/2})$ photofragments through (2 + 1) resonance enhanced multiphoton ionization in a time-of-flight mass spectrometer. Jet cooling reveals two partially resolved bands, which are assigned as transitions to the local-mode $[5,0,0]_{A_1,E}$ and $[3,0,0] + 4\nu_2$ (A_1,E) levels. The ratio of $Cl(^2P_{1/2})$ to $Cl(^2P_{3/2})$ spin–orbit populations was found to be 1.08 ± 0.08 for 238 nm photolysis of vibrationally excited CH_3Cl, significantly larger than the spin–orbit population ratio (0.27 ± 0.01) in Cl fragments from the 235 nm photolysis of ground state CH_3Cl. © 1997 Elsevier Science B.V.

1. Introduction

Exploration of the role vibrational energy can play in altering or controlling the dynamics of photodissociation has continued to be of great interest [1]. The clearest example of this type of mode-selective chemistry involves photodissociation of the HOD molecule, for which excitation of either fundamental or overtone O–H and O–D stretch levels has been shown to lead to preferential cleavage of that bond [2–5]. We might expect that selective modification of the dynamics through vibrational excitation of specific modes would become more difficult in larger molecules because of the more rapid rates of vibrational energy flow in these systems [6]. Nevertheless, changes in the fragment branching ratios and internal state distributions have been observed in the photodissociation of several vibrationally excited tetraatomic molecules, including HNCO [7], C_2HD [8], C_2H_2 [9,10] and H_2O_2 and HOOD [11,12]. In the case of C_2HD, a rotational-state dependent selectivity in the C–H vs. C–D bond fission for excitation of the $5\nu_1$ vibrational level was demonstrated [8].

It is interesting to investigate the vibrationally mediated photodissociation dynamics of even larger molecules. We have begun study of the photodissociation of C–H stretch overtone excited halomethanes, in this study CH_3Cl. It is known that there is strong coupling of the C–H stretch and CH_3 bending modes in the CH_3X systems [13,14], which can impede observation of selectivity in the dynamics. For this reason, there has been more interest in the vibrational overtone spectroscopy and dynamics of CHXYZ type systems, in which the mode coupling is much less [13,15,16]. Nevertheless, for chlorinated methanes, there are several advantages to the study of a molecule such as CH_3Cl. With detection of isotopically selected $^{35,37}Cl$ atomic fragments, iso-

0009-2614/97/$17.00 © 1997 Elsevier Science B.V. All rights reserved.
PII S0009-2614(97)00783-5

topomeric congestion [15] is eliminated. Hippler and Quack [15,17] have investigated the overtone spectrum of $CHCl_3$ in the region of the third C–H stretch overtone transition through isotope-selective detection of Cl atoms formed in the vibrationally mediated photodissociation of this molecule.

The first absorption band of CH_3Cl is featureless, with maximum absorption near 170 nm, and has been assigned to a $\sigma^*_{CCl} \leftarrow$ n transition [18–20]. Excitation to both the $^1Q_1$ and $^3Q_0$ states can occur. Matsumi et al. [21] concluded from Doppler velocity analysis of $Cl(^2P_{3/2,1/2})$ atoms that these fragments are produced in the 193 nm photolysis of ground state CH_3Cl through excitation of the parallel transition to $^3Q_0$. In this communication, we present results from a study of the photodissociation at ≈ 238 nm of CH_3Cl excited to its fourth C–H stretch overtone level [14], with particular emphasis on the ^{35}Cl atom fragments. In a subsequent publication, we will also report our observations on the H and ^{37}Cl atom photofragmentation channels.

2. Experimental

These experiments were carried out in a time-of-flight mass spectrometer (TOFMS) which has been described in detail previously [22]. Fig. 1 presents a schematic diagram of the present experimental arrangement. Two tunable laser beams were employed, specifically near infrared (NIR) laser radiation to prepare CH_3Cl molecules in excited vibrational levels and UV laser radiation both to photodissociate the molecules and to detect atomic fragments by 2 + 1 resonance-enhanced multiphoton ionization (REMPI). In most experiments, the UV laser was fixed on a given atomic transition, while the near infrared laser was tuned across the vibrational band. Methyl chloride (Matheson, 99.5% purity), prepared as a 2–7% mixture in helium at a total pressure of 1–3 atm, was injected with a pulsed valve (General Valve) through a 0.5 mm diameter orifice into the ionization region of the TOFMS. With the beam on, the steady-state pressure in the ionization region was $\approx 3 \times 10^{-5}$ Torr, while the pressure in the differentially pumped flight tube was $\approx 2 \times 10^{-6}$ Torr. Guard electrodes were installed to minimize the distortion of the field in the ionization region from the beam source assembly [22].

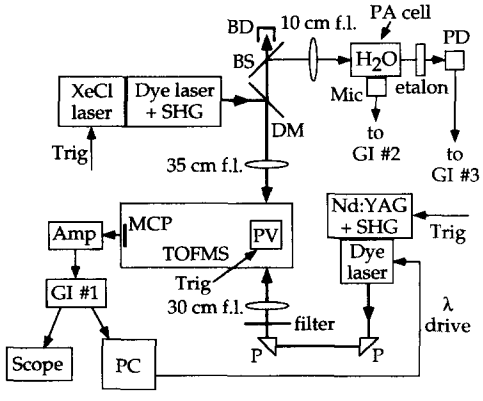

Fig. 1. Schematic diagram of the experimental apparatus. Key to abbreviations: PV, pulsed valve; DM, dichroic mirror; BS, beam splitter; BD, beam dump; P, prism; Mic, microphone; PD, photodiode; GI, gated integrator; MCP, microchannel plates.

Overtone vibrational excitation of CH_3Cl was accomplished by irradiation with the focused (f.l. 30 cm) output (wavelength ≈ 725 nm, pulse energy ≈ 30 mJ, bandwidth ≈ 0.2 cm^{-1}) of a homemade grazing incidence dye laser pumped with the 532 nm output of a Nd:YAG laser (Continuum NY-81C). The counterpropagating uv photolysis/detection laser beam (wavelength 235–239 nm, pulse energy 0.3–1.0 mJ, bandwidth ≈ 0.4 cm^{-1}, obtained from a Lambda Physik excimer laser pumped dye laser system), which was delayed by 20 ns, was focused into the ionization region with a 35 cm f.l. lens. These two laser beams were brought to a common focus in the center of the ionization region of the TOFMS.

The ion signal for a given mass channel was monitored with a gated integrator, whose output was directed to a laboratory computer controlling the data acquisition. In most spectral scans, the NIR laser was fired every other gas pulse, and laser on and off signals were separately summed over a preset number of shots (typically 10–30) before the laser was stepped to the next wavelength. Several diagnostic channels were also recorded during these spectral scans. Wavelength calibration, using the AFGL HITRAN database [23], was provided with a photoacoustic (PA) spectrum [24] of water vapor. A small portion of the NIR laser radiation was focused into a PA cell containing water vapor. Wavenumber differ-

ences were also monitored with a solid fused silica etalon (free spectral range 0.70 cm^{-1}).

In the absence of the overtone laser excitation, the branching ratio for formation of Cl ($^2P_{1/2}$) atoms (denoted hereafter as Cl^*) to that of ground state Cl ($^2P_{3/2}$) (denoted as Cl) was obtained for the photolysis of ground state CH_3Cl. In these experiments, the uv laser was scanned over the atomic Cl transitions while monitoring the laser energy with a pyroelectric detector positioned after the exit window of the ionization chamber. Laser energies were also routinely measured before the chamber with a calorimetric power meter; the two measurements were consistent after taking into account reflection losses at the focusing lens and the chamber windows.

The atomic lines employed for the determination of the Cl^*/Cl branching ratio were the $^2D_{3/2} \leftarrow {}^2P_{3/2}$ and $^2P_{1/2} \leftarrow {}^2P_{1/2}$ transitions at 235.336 and 235.205 nm, respectively. The ratio of the oscillator strengths of these transitions has been measured [25] to be 0.85 to 1. Since calibrated transitions were not required, the Cl and Cl^* photofragment yields from the photolysis of vibrationally excited CH_3Cl as a function of the NIR laser wavenumber were monitored on different atomic transitions, namely $^4D_{5/2} \leftarrow {}^2P_{3/2}$ and $^2D_{5/2} \leftarrow {}^2P_{1/2}$ at 237.733 and 238.770 nm, respectively. We employed these transitions since the dye laser could be operated with a more stable and efficient dye.

As a check on our ability to measure branching ratios, Cl and Cl^* signals were obtained from the 193 nm photolyses of HCl and CH_3Cl, for which previous REMPI measurements of the branching ratios exist [26]. A 5% HCl (Matheson, 99.0% purity) mixture in He was used with backing pressures in the range 500–760 Torr, and with similar chamber pressures as described above for the CH_3Cl/He mixtures. An unpolarized ArF laser (Lambda-Physik Lextra 100) was fired 20–30 ns before the uv laser. A portion of the 193 nm laser beam passed through an iris, limiting the pulse energy to ≤ 50 μJ, and entered the ionization chamber co-propagating with the UV laser. As Cl and Cl^* signals may arise from both the 193 nm and the UV lasers, the 193 nm laser was fired on alternate gas pulses, and the contribution from the UV laser subsequently subtracted. The UV laser and the 193 nm laser beams were separated after the chamber using a 193 nm dichroic mirror and the pulse energies monitored by a pyroelectric detector (UV laser) and a photodiode/sodium salicylate coated window (193 nm laser).

The dependence of the Cl and Cl^* ion signals on the laser energies were determined for the photolysis of ground state HCl and CH_3Cl at 193 nm and at 235 nm. The uv laser was repeatedly scanned over the Cl transitions with either quartz disk attenuators placed in the laser beam or a fine mesh screen attenuator swung into place before the amplifier stage of the UV dye laser. Log–log plots of the Cl peak area against the laser energy yielded slopes of 1.07 ± 0.07 for the 193 nm laser photolysis of HCl, 1.90 ± 0.07 for the UV laser following 193 nm photolysis of HCl, and 2.90 ± 0.02 for the 235 nm photolysis of CH_3Cl. Nearly identical values were obtained for the Cl^* fragment. The squared power dependence for the UV laser is appropriate for REMPI detection (two photon excitation followed by a saturated ionization step) with separate photolysis and probe lasers, while the higher cubic power dependence for 235 nm photolysis arises from the use of a single laser for both photolysis and detection.

The dependence of the Cl^* signal on the pulse energy of the NIR laser was also investigated for the 235 nm photolysis of vibrationally excited CH_3Cl. With the wavelength of the NIR laser tuned to the peak of the overtone spectrum at ≈ 13800 cm^{-1}, the UV laser was scanned repeatedly across the Cl^* REMPI transition while varying the NIR laser energy from 2 to 22 mJ. The slope of the log–log plot of the Cl^* peak area against the NIR laser pulse energy was 1.02 ± 0.02, indicating that the overtone excitation step is a single photon process.

3. Results and discussion

Fig. 2 compares several different types of spectra taken as a function of the NIR laser wavenumber. The top panel displays a PA spectrum of the fourth C–H stretch overtone vibrational transition of CH_3Cl in a room-temperature cell. This spectrum reproduces well the previously reported [14] PA spectrum in this spectral region. The lower panel shows the enhancement of the yield of ^{35}Cl atoms, in both the ground $^2P_{3/2}$ and spin–orbit excited $^2P_{1/2}$ states, from the photolysis of vibrationally excited CH_3Cl

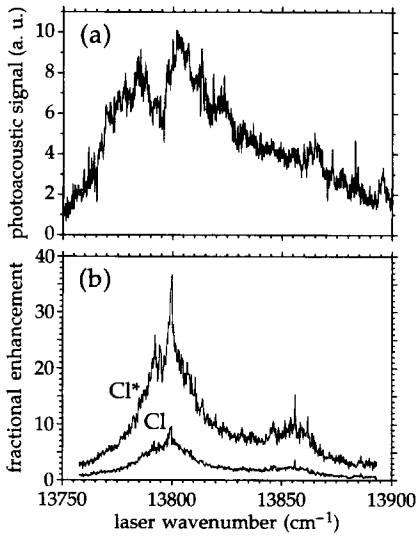

Fig. 2. (a) Room-temperature photoacoustic spectrum of CH_3Cl in the region of the fourth ($v = 5$) overtone C–H stretching transition. (b) Fractional enhancement [defined as $(S_{on} - S_{off})/S_{off}$, where S_{on} and S_{off} are the ion signals with the NIR laser on and off, respectively] of the yield of $^{35}Cl^*$ and ^{35}Cl photofragments as a function of the wavenumber of the NIR laser. As discussed in the text, the wavelength of the UV laser employed for photolysis and ionization was 237.733 and 238.770 nm for Cl and Cl*, respectively. The spacing between adjacent points is 0.3 cm^{-1}.

as the NIR laser is scanned across this band, as compared to the respective yield of Cl and Cl* from photolysis of ground state CH_3Cl. For each spin–orbit level, the exact photolysis wavelength, which is determined by the REMPI transition used to ionize the atoms, is given in the figure caption. No ions were detected with only the NIR laser on.

The Cl and Cl* photofragment yield spectra as a function of the NIR laser wavenumber can be seen in Fig. 2 to be significantly narrower than the room-temperature PA spectrum. This narrowing results from rotational cooling of the CH_3Cl/He mixture in the free jet expansion. We estimate the CH_3Cl rotational temperature to be ≤ 70 K, from diagnostic experiments with H_2O/He beams in which the H atom yield from the 243 nm photodissociation of individual rotational levels of the H_2O $|04\rangle^-$ vibrational state was observed. In contrast to similar studies of $CHCl_3$ overtone spectroscopy [15,27], the intensities of hot bands should be negligible for CH_3Cl since the population of the lowest excited vibrational level (ν_3, at 732.84 cm^{-1} [14]) at room temperature is only 2.9%.

The Cl and Cl* photofragment yield spectra in Fig. 2b appear to have broken up into transitions to two groups of excited levels. By contrast, the room-temperature PA spectrum merely shows a slight asymmetry. Duncan and Law [14] assigned the feature observed in the room-temperature PA spectrum as a transition to the [5,0,0] local mode levels of A_1 and E symmetry. (In the local-mode notation $[v_1,v_2,v_3]$, the three C–H stretch vibrational coordinates possess v_i, $i = 1$–3, quanta of vibration.) The levels of A_1 and E symmetry are degenerate in the local mode limit. A Fermi resonance is known to couple the fundamental ν_1 C–H stretch and $2\nu_5$ bend levels [28]. This coupling becomes very strong in the region of the $v = 3$ C–H stretch levels because of anharmonic tuning of the stretch and bend energies. A close resonance was also observed in the $v = 4$ C–H stretch overtone spectral region and appears to involve a Fermi resonance between ν_1 and $2\nu_2$ [14]. The splitting of the $v = 5$ C–H overtone transition shown in Fig. 2b is again due a Fermi resonance between C–H stretch and bend modes. The vibrational Hamiltonian derived from a fit to the observed CH_3Cl vibrational energies predicts bright levels with significant $[3,0,0] + 4\nu_2$ character of A_1 and E symmetry to occur at 13834 and 13850 cm^{-1}, respectively [29]. The latter wavenumber is near the maximum of the higher-energy set of transitions in Fig. 2b, while the former lies between the two groups of transitions. Since this Hamiltonian was obtained from a fit to the energies of lower vibrational levels, it is not surprising that the agreement with our observations is not perfect.

Superimposed upon the overall band profiles in Fig. 2b are a number of clearly visible sharp band heads. Much of the "noise" in the spectra is reproducible structure. In the slower scans displayed in Fig. 3, partially resolved rotational structure, with a number of the lines having widths comparable to the NIR laser line width, are visible in the spectrum. The spectrum in Fig. 3a is complicated, but that in Fig. 3b shows several features which appear to be red-degraded band heads. In particular, the band near 13847 cm^{-1} is well fit as a Q branch with an upper-state rotational constant of approximately 0.42 cm^{-1}. The spectra of the lower ($v_{C-H} \leq 3$) C–H stretch transi-

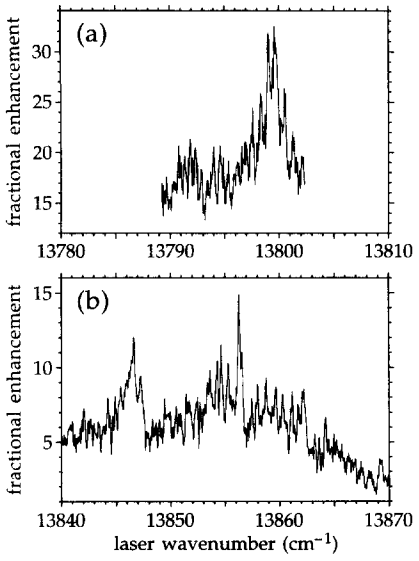

Fig. 3. Higher-resolution scans of selected portions of the $^{35}Cl^*$ enhancement spectrum taken with a smaller step size (0.04 cm^{-1}), showing partially resolved rotational structure.

tions show K subband structure [14], as in the A_1 and E fundamental bands, involving excitation to the different K stacks. There are no banded features in Fig. 2b describable as K subbands. (For survey spectra of the fundamental bands, see ref. [30].) This suggests that the K quantum number is not good at these high levels of vibrational excitation.

We have carefully compared the ratio of Cl^* to Cl enhancements as a function of the NIR laser wavenumber to see if there is a possible dependence of the Cl^* to Cl spin–orbit ratio upon the rotational excitation of the vibrationally excited precursor. The $Cl + CH_3$ exit channel diabatically correlates with the excited $^1Q_1$ state, while $Cl^* + CH_3$ correlates with the $^3Q_0$ state [21]. The ratio of the Cl^* to Cl enhancement was found to equal 4.01 ± 0.04, independent of the laser wavenumber. Thus, there is no detectable precursor rotational state dependence of the fragment spin–orbit population ratio. This suggests that the action spectra in Fig. 2b should be an accurate representation of the overtone absorption spectrum of rotationally cool CH_3Cl in this spectral region.

We see from Fig. 2 that the vibrational enhancement for the Cl^* fragment is significantly greater than for ground-state Cl fragments. We have measured the Cl^*/Cl branching ratio for the photolysis of ground state CH_3Cl by comparing the integrated areas of the Cl^+ ion yields vs. the UV laser wavenumbers and correcting for the previously measured ratio of 2-photon oscillator strengths [25]. We carefully measured the dependence of the ion signals upon the uv laser pulse energy. We then took pains to avoid saturation effects and to normalize the signals for the laser power. As discussed in Section 2, the ion signals scaled in the low-power limit approximately as the cube of the UV laser pulse energy, as expected for 1-photon photolysis, followed by 2-photon excitation of the fragment and a saturated ionization step.

In similar fashion we measured the Cl^*/Cl branching ratios for the 193 nm photolyses of HCl and CH_3Cl. The branching ratios obtained are in good agreement with the results of previous REMPI studies [26] and are listed in Table 1 along with our results of the photolyses of HCl and CH_3Cl at 235 nm. There have been several investigations, both experimental [21,25,26] and theoretical [31–34], of the Cl^*/Cl branching ratio in the photolysis of HCl.

Table 1
Cl^*/Cl branching ratios measured by REMPI detection for the photolysis of HCl and CH_3Cl at several wavelengths

Species	$\lambda_{photolysis}$ (nm)	Total excitation energy (cm^{-1})	Cl^*/Cl ratio	Reference
HCl	193	51800	0.51 ± 0.07	this work
			0.50 ± 0.05	[26]
	235	42550	0.37 ± 0.08	this work
CH_3Cl	157	63700	0.65 ± 0.13	[26]
	193	51500	0.62 ± 0.06	this work
			0.58 ± 0.05	[26]
	235	42550	0.27 ± 0.01	this work
$CH_3Cl^\dagger$	238	55800	1.08 ± 0.08	this work

Our reported value for photolysis at 235 nm is somewhat less than the Cl^*/Cl ratio at 193 nm. The calculations of Alexander et al. [32] predict that the Cl^*/Cl ratio should slowly increase with longer wavelengths.

We obtain a value of 0.27 ± 0.02 for the Cl^*/Cl branching ratio for the photolysis of ground state CH_3Cl at 235 nm. As can be seen from the results presented in Table 1, this is considerably smaller than the ratios determined for photolysis at 193 and 157 nm. Since the Cl atomic spin–orbit splitting is small (881 cm^{-1}, ref. [35]), the ratio of the Cl^* and Cl populations is mainly determined at large CH_3–Cl separations, far from the Franck–Condon region, as demonstrated in quantum flux calculations of the photodissociation of the analogous HCl molecule by Alexander and co-workers [32]. In a semiclassical model of the dissociation dynamics, the Cl^*/Cl branching ratio should depend on the radial velocity in the recoupling region, where the energy separation between potential energy surfaces correlating with the different Cl atomic states is comparable to the spin–orbit energy [32].

If excitation of CH_3Cl at 193 and 235 nm involves a transition to the same single electronically excited state, then we would expect, on the basis of experimental [25] and theoretical [32] Cl^*/Cl branching ratios found for HCl photolysis, a much smaller variation of the Cl^*/Cl ratio than observed (see Table 1) over this range of photolysis energies. As discussed earlier, the Cl atom recoil anisotropy at 193 nm is consistent with excitation to the $^3Q_0$ state [21]. At longer photolysis wavelengths, we might expect that the dissociation dynamics would be more adiabatic. This suggests that Cl^*/Cl ratio should actually be larger at longer photolysis wavelengths, in contrast to the observations, since the $^3Q_0$ state correlates with Cl^* fragments. It thus appears possible that more than one electronic state is accessed in the photodissociation of CH_3Cl.

We have utilized the measured Cl^*/Cl ratio for the 235 nm photolysis of ground state CH_3Cl and the enhancements of the Cl^* and Cl yields for 238 nm photolysis following vibrational excitation to derive Cl^*/Cl fragment yield ratios for the photodissociation of vibrationally excited CH_3Cl. Assuming that photolysis of ground state CH_3Cl at 235 or 238 nm produces similar Cl^*/Cl ratios, we thus calculate a value of 1.08 ± 0.08 for the Cl^*/Cl branching ratio for the 238 nm photolysis of CH_3Cl excited to its fourth overtone level (total excitation energy 55800 cm^{-1}).

If the photolyses of ground and vibrationally excited CH_3Cl involve excitation to a single excited potential energy surface, the Cl^*/Cl ratio should depend mainly on the velocity in the recoupling region, as discussed above. Since the recoupling region is at large separations, where this velocity is close to the asymptotic value, the Cl^*/Cl ratio should depend on the final translational energy, or the total available energy, since the latter appears mainly as translational energy [21]. However, the Cl^*/Cl spin–orbit branching ratio for 235 nm photolysis of vibrationally excited CH_3Cl is dramatically greater than the ratios determined for 1-photon 193 and 157 nm photolysis of ground state CH_3Cl, despite similar excitation energies (see Table 1). This strongly suggests that other factors beside the velocity in the recoupling region is determining the fragment spin–orbit branching in the photolysis of the vibrationally excited molecule. This modification of the dissociation dynamics could be the result of accessing different regions of the excited potential energy surface(s), or differences in the electronic states initially excited. In future experiments, we hope to clarify the dynamics of the ground and excited state photolyses through measurement of vector correlations and energy disposal of the fragments.

4. Conclusion

In this Letter, we have shown that vibrational excitation in the fourth C–H stretch overtone greatly enhances the yield of Cl fragments in the photolysis of CH_3Cl in the long wavelength tail of its first absorption band, near 238 nm. With rotational cooling, this vibrational transition has separated into two peaks. The most intense one is assigned as transitions to A_1 and E levels of predominantly [5,0,0] local mode character, while the weaker peak involves excitation of levels of $[3,0,0] + 4\nu_2$ character.

The most interesting observation of this study is the markedly different Cl^*/Cl spin–orbit branching ratio for photolysis of vibrationally excited molecules

than for photolysis of ground state CH_3Cl. Thus the photodissociation dynamics has been significantly altered, despite the fact that the bond being broken is not directly involved in the initial vibrational excitation. It will be interesting to compare the Cl and H photofragmentation channels, as well as to study the photofragmentation as a function of the photolysis wavelength and polarization.

Acknowledgements

We are grateful to I. Bar and S. Rosenwaks for useful communications and advice concerning the optimization of the vibrationally enhanced signal and for a critical reading of the manuscript. We also acknowledge M. Kawasaki for helpful correspondence about Cl REMPI line strength factors and M.M. Law for sending us the results of unpublished calculations of CH_3Cl vibrational energies. This research has been supported by the US Army Research Office, under grant No. DAAH04-95-1-0128, and by the National Science Foundation, under grant No. CHE-9313722. Travel support has been provided by the US–Israel Binational Science Foundation.

References

[1] F.F. Crim, J. Phys. Chem. 100 (1996) 12725.
[2] R.L. Vander Wal, J.L. Scott, F.F. Crim, J. Chem. Phys. 92 (1990) 803.
[3] V. Engel, V. Staemmler, R.L. Vander Wal, F.F. Crim, R.J. Sension, B.J. Hudson, P. Andresen, S. Hennig, K. Weide, R. Schinke, J. Phys. Chem. 96 (1992) 3201.
[4] I. Bar, Y. Cohen, D. David, S. Rosenwaks, J.J. Valentini, J. Chem. Phys. 93 (1990) 2146.
[5] Y. Cohen, I. Bar, S. Rosenwaks, J. Chem. Phys. 102 (1995) 3612.
[6] D.J. Nesbitt, R.W. Field, J. Phys. Chem. 100 (1996) 12735.
[7] S.S. Brown, R.B. Metz, H.L. Berghout, F.F. Crim, J. Chem. Phys. 105 (1996) 6293.
[8] T. Arusi-Parpar, R.P. Schmid, R.-J. Li, I. Bar, S. Rosenwaks, Chem. Phys. Lett. 268 (1997) 163.
[9] J. Zhang, C.W. Riehn, M. Dulligan, C. Wittig, J. Chem. Phys. 103 (1995) 6815.
[10] R.P. Schmid, T. Arusi-Parpar, R.-J. Li, I. Bar, S. Rosenwaks, J. Chem. Phys. 107 (1997) xxxx.
[11] M. Brouard, M.T. Martinez, J. O'Mahony, J.P. Simons, J. Chem. Soc. Faraday Trans. 285 (1989) 1207.
[12] M. Brouard, M.T. Martinez, J. O'Mahony, J.P. Simons, Mol. Phys. 69 (1990) 65.
[13] M. Quack, Annu. Rev. Phys. Chem. 41 (1990) 839.
[14] J.L. Duncan, M.M. Law, J. Mol. Spectrosc. 140 (1990) 13.
[15] M. Hippler, M. Quack, J. Chem. Phys. 104 (1996) 7426.
[16] O.V. Boyarkin, T.R. Rizzo, J. Chem. Phys. 105 (1996) 6285.
[17] M. Hippler, M. Quack, Chem. Phys. Lett. 231 (1994) 75.
[18] R.S. Mulliken, J. Chem. Phys. 8 (1940) 328.
[19] A. Gedanken, M.D. Rowe, Chem. Phys. Lett. 34 (1975) 39.
[20] D. Nachtigallova, D.E. Love, K.D. Jordan, J. Phys. Chem. 100 (1996) 5642.
[21] Y. Matsumi, P.K. Das, M. Kawasaki, J. Chem. Phys. 92 (1990) 1696.
[22] D.F. Varley, P.J. Dagdigian, J. Phys. Chem. 99 (1995) 9843.
[23] L.S. Rothman, R.R. Gamache, R.H. Tipping, C.P. Rinsland, M.A.H. Smith, D.C. Brenner, V. Malathy Devi, J.-M. Flaud, C. Camy-Peyret, A. Perrin, A. Goldman, S.T. Massie, L.R. Brown, R.A. Toth, J. Quant. Spectrosc. Radiat. Transfer 48 (1992) 469.
[24] G.A. West, J.J. Barrett, D.R. Siebert, K.V. Reddy, Rev. Sci. Instrum. 54 (1983) 797.
[25] R. Liyanage, Y. Yang, S. Hashimoto, R.J. Gordon, R.W. Field, J. Chem. Phys. 103 (1995) 6811.
[26] Y. Matsumi, P.K. Das, M. Kawasaki, K. Tonokura, T. Ibuki, G. Inoue, S. Satyapal, R. Bersohn, J. Chem. Phys. 97 (1992) 5261.
[27] M. Hippler, M. Quack, Ber. Bunsenges. Phys. Chem. 99 (1995) 417.
[28] N. Bensari-Zizi, C. Alamichel, J. Mol. Spectrosc. 99 (1983) 98.
[29] M.M. Law, Ph.D. Thesis, Aberdeen University (1992).
[30] J.W. Elkins, R.H. Kagann, R.L. Sams, J. Mol. Spectrosc. 105 (1984) 480.
[31] S.C. Givertz, G. Balint-Kurti, J. Chem. Soc. Faraday Trans. 282 (1986) 1231.
[32] M.H. Alexander, B. Pouilly, T. Duhoo, J. Chem. Phys. 99 (1993) 1752.
[33] I.H. Gersonde, S. Henig, H. Gabriel, J. Chem. Phys. 101 (1994) 9558.
[34] T. Duhoo, B. Pouilly, J. Chem. Phys. 103 (1995) 182.
[35] C.E. Moore, Atomic Energy Levels, NSRDS-NBS 35 (U.S. Government Printing Office, Washington, 1971).